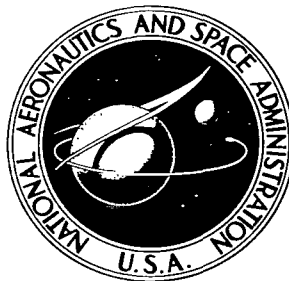


NASA TECHNICAL NOTE



NASA TN D-3344

c. 1

NASA TN D-3344

LOAN COPY: RETURN TO  
AFWL (WLIL-2)  
KIRTLAND AFB, N MEX

0130623



TECH LIBRARY KAFB, NM

# CURRENT DISTRIBUTION IN A THIN FILM SUPERCONDUCTING STRIP TRANSMISSION LINE

*by A. R. Sass and I. D. Skurnick*

*Lewis Research Center*

*Cleveland, Ohio*

NATIONAL AERONAUTICS AND SPACE ADMINISTRATION • WASHINGTON, D. C. • MARCH 1966





CURRENT DISTRIBUTION IN A THIN FILM SUPER-  
CONDUCTING STRIP TRANSMISSION LINE

By A. R. Sass and I. D. Skurnick

Lewis Research Center  
Cleveland, Ohio

NATIONAL AERONAUTICS AND SPACE ADMINISTRATION

For sale by the Clearinghouse for Federal Scientific and Technical Information  
Springfield, Virginia 22151 - Price \$0.40

# CURRENT DISTRIBUTION IN A THIN FILM SUPER- CONDUCTING STRIP TRANSMISSION LINE\*

by A. R. Sass<sup>†</sup> and I. D. Skurnick

Lewis Research Center

## SUMMARY

In the long wavelength limit the current distribution in a thin film superconducting strip transmission line can be described by an inhomogeneous Fredholm integral equation of the second kind. When a fluxoid conservation derivation of this equation is considered, physical insight into the structure of the kernel follows naturally. An approximate analytic solution to the integral equation is derived for a specified range of geometrical parameters commonly encountered in practice. The solution is obtained by making use of the Liouville-Neumann method of successive approximations, and by approximating the resulting series by a series involving powers of a defined coupling factor. It is shown that the critical current of the thin film superconducting strip transmission line, based on the calculations in this report and a critical current density hypothesis, is underestimated by less than 10 percent.

## INTRODUCTION

Several authors have indicated that superconductive computer components, which are constructed in the form of thin film strip transmission lines, are advantageous from the standpoint of switching speed and miniaturization (refs. 1 to 6). Superconducting strip transmission lines are also useful in the transportation of electrical information within a superconducting computer due to inherent negligible loss characteristics and high group velocity (refs. 2 and 5). The latter is true only if the film thickness is larger than, or comparable to, the London penetration depth. It has also been shown that if the film

---

\*A condensed version of this report was published in J. Appl. Phys., vol. 36, no. 7, July 1965, pp. 2260-2267.

<sup>†</sup>Presently employed at the RCA Laboratories, Princeton, New Jersey.

thickness is less than the penetration depth the group velocity is appreciably decreased, which makes the strip line useful for delay line memory application (ref. 2). In all these devices it would be useful to be able to predict the total current which can be carried by the strip line before it becomes normally conducting.

Several microscopic theories have been advanced which indicate that switching in a thin film is initiated by a critical current density (ref. 7). Cooper and Marcus have shown, independently, that the problem of thin film switching is complicated by the fact that the current density is not constant over the cross section of the film (refs. 8 to 10). By using a formal Green's function approach and employing the London current-field relation, Cooper derived the general inhomogeneous Fredholm integral equation of the second kind describing the current density distribution in a single film. He also obtained a specialized equation for the case in which the film thickness is less than or equal to the penetration depth - the thin film case. Marcus derived an identical equation by combining the Biot-Savart law and the London equation, and obtained computer solutions for the thin film case. These methods can be used to derive an integral equation for the current distribution in a strip transmission line. Due to the complexity of the kernel, analytic solutions to the integral equation have not been found to date for either the single film or strip line cases.

It will be shown that when the integral equation is derived for the superconducting strip transmission line, by using the concept of fluxoid conservation and the London current-field relation, certain useful properties of the kernel can be readily deduced. The integral equation is solved by using the Liouville-Neumann method of successive approximations. The properties of the kernel allow the approximate evaluation of the Liouville-Neumann series for a range of geometric parameters of practical interest. The analytic solution for the current density distribution in the strip line exhibits the same property of current peaking at the film edges that Cooper and Marcus found for the single film. The critical current of the system can be calculated from a knowledge of the current density in the strip line and the critical current density obtained from microscopic theory and/or independent experimentation.

## SYMBOLS

The rationalized mks system of units is employed throughout the report.

$\hat{a}$	unit vector
$\vec{B}$	magnetic induction
C	constant determined by total current

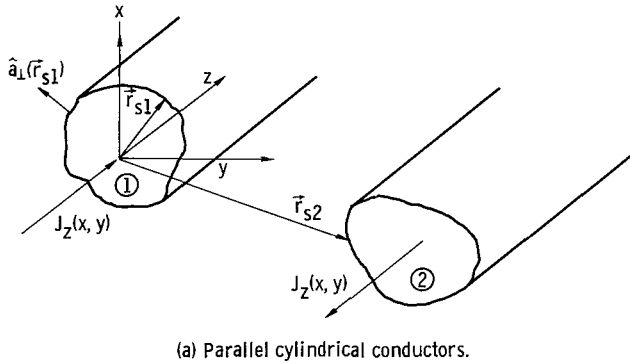
$d$	thickness of film
$\vec{E}$	electric field intensity
$G(x', y - y')$	$\int \ln \left  (x')^2 + (y - y')^2 \right  dx'$
$\vec{H}$	magnetic field intensity
$\vec{H}_{ij}$	magnetic field intensity at point $i$ due to current element at point $j$
$I$	total current
$\vec{J}$	current per unit area
$\vec{J}_w$	current per unit width
$K(u, u')$	kernel of one dimensional Fredholm integral equation
$k$	$\ell/d$
$\ell$	distance between centers of two films in a strip-line pair
$\vec{r}$	field point in x-y plane
$\vec{r}'$	source point in x-y plane
$\vec{r}_s$	position vector denoting surface of conductor
$t$	time
$u$	$\frac{2}{w} y$ dimensionless field point in one-dimensional analysis
$u'$	$\frac{2}{w} y'$ dimensionless source point in one-dimensional analysis
$w$	width of film
$\beta^{-1}$	London penetration depth
$\kappa(u)$	coupling factor = $\int_{-1}^1 K(u, u') du'$
$\lambda$	$(\beta d)^2 (w/d) / 8\pi$
$\mu_0$	permeability of free space, $4\pi \times 10^{-7}$ H/m
$\sigma$	electrical conductivity measured in mho/m
$\chi_m$	magnetic susceptibility

## STATEMENT OF PROBLEM

It will be interesting to compare some general features of the current distribution in a strip transmission line for the cases where (1) the conductors are both normally conducting, (2) both conductors are superconducting, and (3) one conductor is superconducting and the other is normally conducting. Consider the line structure in the form of two parallel cylindrical conductors shown in figure 1(a). For the sake of generality it is assumed, at first, that the cross section of each conductor is arbitrary. It is further assumed that (a) the wavelengths of the fields propagating along the structure are much larger than the transverse dimensions of the system so that a quasi-static analysis is valid, and (b) the current density is in the z-direction and therefore is only a function of x and y. The latter condition is a consequence of charge conservation for the quasi-static case ( $\nabla \cdot \vec{J} \approx 0$ ).

It is convenient to first discuss the situation in which both cylinders are normally conducting. Faraday's induction law, expressed in integral form, is

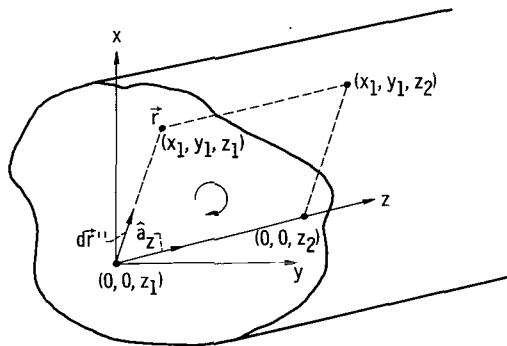
$$\oint \vec{E} \cdot d\vec{s} = - \frac{d}{dt} \iint \vec{B} \cdot d\vec{S} \quad (1)$$



where  $d\vec{s}$  is an element of the contour bounding an area  $\vec{S}$ . Since  $\vec{J} = \sigma \vec{E}$  in both conductors and  $\chi_m \ll 1 \approx 10^{-5}$  for most ordinary paramagnetic and diamagnetic materials, equation (1) can be rewritten as

$$\oint \vec{J} \cdot d\vec{s} = - \sigma \mu_0 \frac{d}{dt} \iint \vec{H} \cdot d\vec{S} \quad (2)$$

Applying Faraday's law to the dotted contour in figure 1(b) and letting the path in the z-direction be of unit length yield



$$J(\vec{r}) - J(0) = \sigma \mu_0 \frac{d}{dt} \int_0^{\vec{r}} \vec{H}(\vec{r}''') \cdot (\hat{a}_z \times d\vec{r}''') \quad (3)$$

where  $\vec{r}$  is the usual position vector in the x-y plane,  $\hat{a}_z$  is a unit vector in

Figure 1. - Array of infinitely long cylindrical superconductors.

the z-direction, and  $d\vec{r}'$  is a differential vector line element of integration. The magnetic field intensity at the point  $\vec{r}'$  generated by current elements in both conductors is  $\vec{H}(\vec{r}')$ . For the static case, the right-hand side of equation (3) is zero and therefore the current distribution in each conductor is uniform. It is interesting to note that the distribution in a normal conductor is uniform even if the neighboring conductor does not have a uniform distribution. An example of this point is the situation where the second conductor is a superconductor. This case will be described later in the report.

For the case in which both conductors are perfectly conducting ( $\sigma = \infty$ ), the right-hand side of equation (3) is still zero in the static situation. However, at some time in the past a transient existed so that it appears that infinite current densities were generated. This unrealistic situation is alleviated by stipulating that during the transient and afterwards the current flows in an infinitely thin layer at the perfect conductor surfaces with a distribution such that  $\vec{H}$  is time independent everywhere inside the body of the conductor. Starting from zero field initial conditions it is evident that  $\vec{H}$  is zero everywhere inside of the cylinders. Thus the magnetic flux through any imaginary surface in the interior of either conductor is zero. It is easy to show that the magnetic field at a point  $\vec{r}$  in a cross section, due to an infinitely long line current  $I$ , which intersects the plane of the cross section at  $\vec{r}'$  is given by

$$\vec{H}(\vec{r}) = \frac{I}{2\pi} \frac{\hat{a}_z \times (\vec{r} - \vec{r}')}{|\vec{r} - \vec{r}'|^2} \quad (4)$$

If there is to be no component of  $\vec{H}(\vec{r})$  perpendicular to the surfaces, then at every point on the surfaces of both cylinders it must be true that

$$\vec{H}(\vec{r}_{s1,2}) \cdot \hat{a}_1(\vec{r}_{s1,2}) = 0$$

where  $\vec{r}_{s1}$  and  $\vec{r}_{s2}$  are the position vectors denoting the surface of conductors 1 and 2, respectively, and  $\hat{a}_1(\vec{r}_{s1,2})$  is the unit vector normal to the surface of the conductors.

Since  $\vec{H}(\vec{r}_{s1,2})$  is found by summing over the contribution to the field made by current elements at the surfaces of both cylinders, it follows that  $\vec{H}$  vanishes everywhere inside of the cylinders if  $\vec{J}_w(\vec{r}_s)$ , the current per unit width at the conductor surface, is the solution to the pair of coupled integral equations

$$\left. \begin{aligned}
& \int_{\textcircled{1}} \frac{J_w(\vec{r}'_{s1}) [\hat{a}_z \times (\vec{r}_{s1} - \vec{r}'_{s1}) \cdot \hat{a}_\perp(\vec{r}'_{s1})]}{2\pi |\vec{r}_{s1} - \vec{r}'_{s1}|^2} dr'_{s1} \\
& - \int_{\textcircled{2}} \frac{J_w(\vec{r}'_{s2}) [\hat{a}_z \times (\vec{r}_{s1} - \vec{r}'_{s2}) \cdot \hat{a}_\perp(\vec{r}'_{s1})]}{2\pi |\vec{r}_{s1} - \vec{r}'_{s2}|^2} dr'_{s2} = 0 \\
& \int_{\textcircled{1}} \frac{J_w(\vec{r}'_{s1}) [\hat{a}_z \times (\vec{r}_{s2} - \vec{r}'_{s1}) \cdot \hat{a}_\perp(\vec{r}'_{s2})]}{2\pi |\vec{r}_{s2} - \vec{r}'_{s1}|^2} dr'_{s1} \\
& - \int_{\textcircled{2}} \frac{J_w(\vec{r}'_{s2}) [\hat{a}_z \times (\vec{r}_{s2} - \vec{r}'_{s2}) \cdot \hat{a}_\perp(\vec{r}'_{s2})]}{2\pi |\vec{r}_{s2} - \vec{r}'_{s2}|^2} dr'_{s2} = 0
\end{aligned} \right\} \quad (5)$$

While these equations will not be solved here, two interesting consequences are apparent from their form alone.

(1) The surface current distribution in conductor 1 is influenced by the cross-sectional shape of conductor 1, conductor 2, and the separation between them.

(2) The surface current distribution in conductor 1 depends on the distribution in conductor 2. The distribution in conductor 1 is altered by the presence of conductor 2 even if conductor 2 carries zero net current.

The static case in which  $\sigma = \infty$  can be simulated by a dynamic situation in which the skin depth is much less than the transverse dimensions of the conductor.

Consider the case in which both conductors are superconducting. In this situation it is no longer correct to use the expression  $\vec{J} = \sigma \vec{E}$ , but instead the phenomenological equation of F. and H. London should be employed. Thus,

$$\vec{E} = \mu_0 \beta^{-2} \frac{\partial \vec{J}}{\partial t} \quad (6)$$

The parameter  $\beta^{-1}$  is the London penetration depth, the distance through which the magnetic field falls to  $1/e$  of its value at the surface of a superconducting half-space. It follows from equations (1) and (6) that

$$\frac{d}{dt} \left[ \vec{J}(\vec{r}) - \vec{J}(0) - \beta^2 \int_0^{\vec{r}} \vec{H}(\vec{r}'') \cdot (\hat{a}_z \times d\vec{r}'') \right] = 0 \quad (7)$$

The quantity within the brackets in equation (7) is the well-known London fluxoid. Thus, equation (7) expresses the principle of fluxoid conservation. Starting from the London zero field initial conditions, it is seen that the fluxoid associated with this or any other contour within the superconducting cylinder is zero. This is the exact analog of the zero flux condition encountered in the case of perfect conductors. Conclusions 1 and 2 which were stated for perfect conductors remain the same for superconductors except that the word surface must be deleted. This is apparent since the infinite current density situation associated with a time rate of change of flux no longer exists in this case.

The magnetic field at a point  $\vec{r}''$  in either cylinder can readily be found by summing over the contributions made by the current elements in both cylinders. Clearly then

$$\vec{H}(\vec{r}'') = \int_{\textcircled{1}, \textcircled{2}} \frac{J(\vec{r}') [\hat{a}_z \times (\vec{r}'' - \vec{r}')] d^2\vec{r}'}{2\pi |\vec{r}'' - \vec{r}'|^2} \quad (8)$$

But

$$\frac{\vec{r}'' - \vec{r}'}{|\vec{r}'' - \vec{r}'|^2} = + \nabla \ln |\vec{r}'' - \vec{r}'|$$

where  $\nabla$  operates on the field point variables. Therefore,

$$\vec{H}(\vec{r}'') = \int_{\textcircled{1}, \textcircled{2}} J(\vec{r}') \left( \frac{\hat{a}_z}{2\pi} \times \nabla \ln |\vec{r}'' - \vec{r}'| \right) d^2\vec{r}' \quad (9)$$

When use is made of the vector identity

$$\nabla \times S\vec{V} = S(\nabla \times \vec{V}) + \nabla S \times \vec{V}$$

it follows that

$$\vec{H}(\vec{r}'') = \int_{\textcircled{1}, \textcircled{2}} J(\vec{r}') \nabla \times \left( -\frac{\hat{a}_z}{2\pi} \ln |\vec{r}'' - \vec{r}'| \right) d^2\vec{r}' \quad (10)$$

Since the integration is being performed over the source points, and  $\nabla \times$  operates only on field points, the curl operator can be taken out from under the integral sign. Hence in the cylinders,

$$\vec{H}(\vec{r}'') = \nabla \times \left[ -\frac{\hat{a}_z}{2\pi} \int_{\textcircled{1}, \textcircled{2}} J(\vec{r}') \ln |\vec{r}'' - \vec{r}'| d^2\vec{r}' \right] \quad (11)$$

It should be noted that equation (11) could also have been derived by first determining the vector potential for the system. If the vector potential  $\vec{A}$  satisfies the requirements of the Coulomb gauge ( $\nabla \cdot \vec{A} = 0$ ), it can be shown that  $\mu_0^{-1} \vec{A}$  is just the expression contained within the brackets in equation (11). Using the identity

$$\vec{H}(\vec{r}'') \cdot (\hat{a}_z \times d\vec{r}'') = \frac{1}{2\pi} \frac{\partial}{\partial r''} \int_{\textcircled{1}, \textcircled{2}} J(\vec{r}') \ln |\vec{r}'' - \vec{r}'| d^2\vec{r}' dr'' \quad (12)$$

and the fact that the fluxoid is zero yield

$$J(\vec{r}) = J(0) - \frac{\beta^2}{2\pi} \int_{\textcircled{1}, \textcircled{2}} J(\vec{r}') \ln |\vec{r}''| d^2\vec{r}' + \frac{\beta^2}{2\pi} \int_{\textcircled{1}, \textcircled{2}} J(\vec{r}') \ln |\vec{r} - \vec{r}'| d^2\vec{r}' \quad (13)$$

Equation (13) is equivalent to that derived by Cooper and Marcus. The first two terms on the right-hand side are independent of  $\vec{r}$ , therefore the current density can be expressed as

$$J(\vec{r}) = C + \frac{\beta^2}{2\pi} \int_{\textcircled{1}, \textcircled{2}} J(\vec{r}') \ln |\vec{r} - \vec{r}'| d^2\vec{r}' \quad (14)$$

where  $C$  is an arbitrary constant determined by the total current.

When the steps in this derivation are reconsidered, the following interesting fact is apparent: The nonuniformity of the current density in the film ( $J(\vec{r}) \neq J(0)$ ,  $\vec{r} \neq 0$ ) is due to the magnetic flux crossing the area bounded by the dotted contour shown in figure 1(b). For certain cross-sectional geometries, such as the strip transmission line which will be discussed later, this flux is small if the conductors carry equal but oppositely directed currents. Thus, in these cases, only small variations of the current density are expected. Furthermore, in the case of a strip transmission line, this concept allows certain properties of the kernel of the integral equation to be deduced so that a closed form solution to equation (14) can be demonstrated.

Before proceeding to this solution, consider the case in which conductor 1 is superconducting and conductor 2 is normally conducting. As was shown previously, the current density in the normal conductor is uniform (in the static case) so that if  $I_{1,2}$  are the net currents in conductors 1 and 2, respectively, equation (13) becomes

$$\begin{aligned}
J(\vec{r}) - J(0) = & \frac{\beta^2}{2\pi} \int_{\textcircled{1}} J(\vec{r}') \ln |\vec{r} - \vec{r}'| d^2\vec{r}' - \frac{\beta^2}{2\pi} \int_{\textcircled{1}} J(\vec{r}') \ln |r'| d^2\vec{r}' \\
& + \frac{\beta^2 I_2}{2\pi S_2} \int_{\textcircled{2}} \ln |\vec{r} - \vec{r}'| d^2\vec{r}' - \frac{\beta^2 I_2}{2\pi S_2} \int_{\textcircled{2}} \ln |\vec{r}'| d^2\vec{r}' \quad (15)
\end{aligned}$$

It is interesting to note that for this case the distribution of the current in conductor 1 is not influenced by the presence of conductor 2 for  $I_2 = 0$ . This was not true for the case of two perfect conductors or two superconductors, as was shown previously.

## STRIP TRANSMISSION LINE OF RECTANGULAR CROSS SECTION

Consider the strip transmission line, shown in figure 2, that consists of two parallel, infinitely long, superconducting thin films of rectangular cross section. Each is of width  $w$  and thickness  $d$ , and the centers of the two are separated by a distance  $\ell$ .

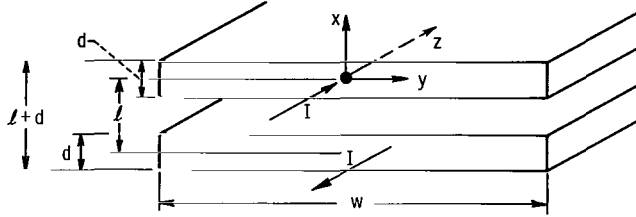


Figure 2. - Strip transmission line.

The parameters of the system are chosen to be in a range of practical interest characterized by  $0.0001 \leq d/w \leq 0.01$ , and  $(\beta d) \leq 1$ . A current  $I$  flows into the top film, and an equal but oppositely directed current flows in the bottom film. For the case of the strip transmission line system just described, equation (14) becomes

$$\begin{aligned}
J(x, y) = C + \frac{\beta^2}{4\pi} & \left[ \int_{-w/2}^{w/2} \int_{-d/2}^{d/2} J(x', y') \ln |(x - x')^2 + (y - y')^2| dx' dy' \right. \\
& \left. + \int_{-w/2}^{w/2} \int_{-(d/2)-\ell}^{(d/2)-\ell} J(x', y') \ln |(x - x')^2 + (y - y')^2| dx' dy' \right] \quad (16a)
\end{aligned}$$

Using the change of variables  $x' \rightarrow -(x' + \ell)$  in the last integral on right-hand side in equation (16a) and noting that

$$J(x, y) \Big|_{-\frac{d}{2} < x < \frac{d}{2}} = -J(-x-\ell, y) \Big|_{-\frac{d}{2} < x < \frac{d}{2}} \quad (16b)$$

yield

$$J(x, y) = C + \frac{\beta^2}{4\pi} \int_{-w/2}^{w/2} \int_{-d/2}^{d/2} J(x', y') \ln \frac{|(x - x')^2 + (y - y')^2|}{|(x + x' + \ell)^2 + (y - y')^2|} dx' dy' \quad (17)$$

Since  $(\beta d) \leq 1$  it will be assumed that  $J$  does not vary appreciably in the  $x$ -direction in the film. (This assumption will be examined more closely in the next section.) Therefore,  $J(x, y) \approx J(0, y) = J(y)$ . It is convenient in equation (17) to perform the integration over  $x'$  first. Let

$$G(x', y-y') = \int \ln |(x')^2 + (y - y')^2| dx' = x' \ln |(x')^2 + (y - y')^2| - 2x' + 2(y - y') \tan^{-1} \frac{x'}{y - y'}$$

Then,

$$\int_{-d/2}^{d/2} \ln \frac{|(x')^2 + (y - y')^2|}{|(x' + \ell)^2 + (y - y')^2|} dx' = G \Big|_{-\frac{d}{2}}^{\frac{d}{2}} - G \Big|_{-\frac{d}{2}}^{\ell + \frac{d}{2}} \quad (18)$$

Thus,

$$J(y) = C + \frac{\beta^2}{4\pi} \int_{-w/2}^{w/2} J(y') dy' \left\{ \left[ d \ln \left| \frac{d^2}{4} + (y - y')^2 \right| - 2d + 4(y - y') \tan^{-1} \frac{d/2}{y - y'} \right] - \left[ \left( \ell + \frac{d}{2} \right) \ln \left| \left( \ell + \frac{d}{2} \right)^2 + (y - y')^2 \right| \right. \right. \\ \left. \left. - 2 \left( \ell + \frac{d}{2} \right) + 2(y - y') \tan^{-1} \left( \frac{\ell + \frac{d}{2}}{y - y'} \right) - \left( \ell - \frac{d}{2} \right) \ln \left| \left( \ell - \frac{d}{2} \right)^2 + (y - y')^2 \right| + 2 \left( \ell - \frac{d}{2} \right) - 2(y - y') \tan^{-1} \left( \frac{\ell - \frac{d}{2}}{y - y'} \right) \right] \right\} \quad (19)$$

When the dimensionless variable  $u = \frac{2}{w} y$  is introduced, equation (19) becomes

$$J(u) = C + \frac{(\beta d)^2 \left(\frac{w}{d}\right)}{8\pi} \int_{-1}^1 J(u') K(u, u') du' \quad (20a)$$

where

$$\begin{aligned} K(u, u') = K(|u - u'|) = & \ln \left| \left(\frac{d}{w}\right)^2 + (u - u')^2 \right| + 2 \frac{u - u'}{d/w} \tan^{-1} \left( \frac{d/w}{u - u'} \right) \\ & + \frac{1}{d} \left[ \left(\ell - \frac{d}{2}\right) \ln \left| \left(2 \frac{\ell}{w} - \frac{d}{w}\right)^2 + (u - u')^2 \right| \right. \\ & \left. - \left(\ell + \frac{d}{2}\right) \ln \left| \left(2 \frac{\ell}{w} + \frac{d}{w}\right)^2 + (u - u')^2 \right| \right] + \frac{u - u'}{d/w} \left[ \tan^{-1} \left( \frac{2 \frac{\ell}{w} - \frac{d}{w}}{u - u'} \right) - \tan^{-1} \left( \frac{2 \frac{\ell}{w} + \frac{d}{w}}{u - u'} \right) \right] \end{aligned} \quad (20b)$$

The kernel of the integral equation is an explicit function of the thickness to width ratio of the films, as well as the ratio of the separation distance to the width. It was mentioned earlier that the nonuniformity of the current density is due to the magnetic flux that crosses the area bounded by the dotted contour shown in figure 1(b). Certainly line currents (henceforth referred to as source points since the analysis is two dimensional) at all points in the cross section contribute to the total flux. In figure 3 let the

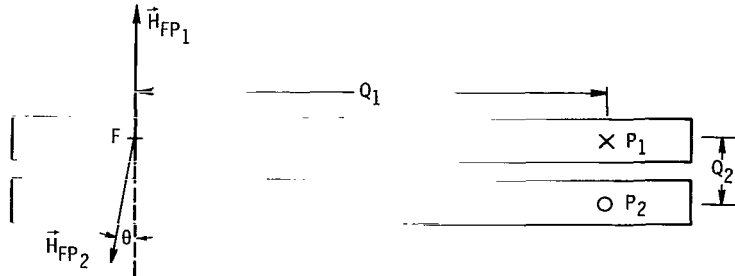


Figure 3. - Flux contributions from antisymmetric source points.

currents at  $P_1$  and  $P_2$  be equal in magnitude but oppositely directed. Let  $Q_1$  be the distance between points  $F$  and  $P_1$ , and  $Q_2$  be the distance between points  $P_1$  and  $P_2$ .

If  $\vec{H}_{FP_1}$  and  $\vec{H}_{FP_2}$  are the magnetic field components at  $F$  due to the currents at  $P_1$  and  $P_2$ , respectively, then if  $Q_1 \geq 7Q_2$ ,

$$\frac{|\vec{H}_{FP_1}| - |\vec{H}_{FP_2}|}{|\vec{H}_{FP_1}|} \leq 0.01$$

and

$$0.989 < \cos \theta < 1.000$$

Thus, due to the dimensions of the transmission line that are being considered, contributions from antisymmetric source points (in the two films) at large distances from the observation point tend to cancel themselves out. It should be expected, therefore, that virtually the entire net flux will be contributed by source points that lie within some small distance from the observation point ( $x, y$ ). This distance should be of the order of  $10 \ell$ , where  $\ell$  is the separation distance between the two films. Thus the kernel should be sharply peaked about  $u = u'$  and, based on the preceding discussion, it should be expected that the magnitude of the kernel will be a monotonically decreasing function of  $|u - u'|$ . Since  $\ell > d$  and  $-(d/2) \leq x, x' \leq (d/2)$ , the two-dimensional kernel in equation (17) is negative definite. When the process is considered by which equation (20a) is derived from equation (17), it is apparent that the one-dimensional kernel in equation (20b) is also negative definite.

A plot of the absolute magnitude of the dimensionless kernel against  $(u - u')$ , which

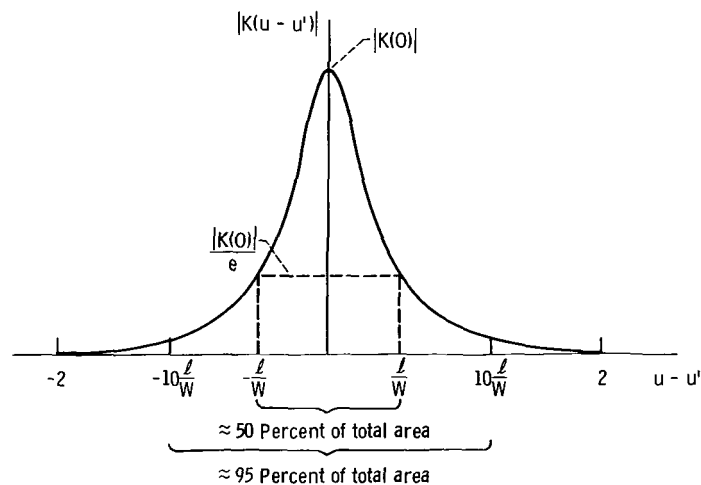


Figure 4. - Absolute value of kernel of inhomogeneous integral equation (not to scale).

summarizes the conclusions of the previous discussion, is shown in figure 4. This approximate sketch is supported by numerical analysis and shows that the kernel drops off to  $\approx 1/e$  of its maximum value when  $|u - u'|$  is on the order of  $\ell/w$ , and that the bulk of the area under the curve (95 percent) is contained in the interval  $0 \leq |u - u'| \leq 10(\ell/w)$ . Note that approximately 50 percent of the area under the curve is contained in the range  $0 \leq |u - u'| \leq (\ell/w)$ .

If

$$\lambda = \frac{(\beta d)^2 \left(\frac{w}{d}\right)}{8\pi} \quad (21a)$$

equation (20a) can be rewritten as

$$J(u) = C - \lambda \int_{-1}^1 J(u') |K(|u - u'|)| du' \quad (21b)$$

Equation (21b) can be solved by the Liouville-Neumann method of successive approximations. Let  $J_0(u) = C$ . Carrying through the integration on the right-hand side in equation (21b) yields

$$J_1(u) = C \left[ 1 - \lambda \int_{-1}^1 |K(|u - u_1|)| du_1 \right] \quad (22a)$$

Repeating the process a second time but now inserting  $J_1(u)$  in the integrand of the right-hand member yields

$$J_2(u) = C \left[ 1 - \lambda \int_{-1}^1 |K(|u - u_1|)| du_1 + \lambda^2 \int_{-1}^1 \int_{-1}^1 |K(|u_1 - u_2|)| |K(|u - u_1|)| du_2 du_1 \right] \quad (22b)$$

Thus, after  $n$  repetitions it can be shown that

$$J_n(u) = C \left[ 1 + \sum_{m=1}^n (-\lambda)^m \int_{-1}^1 \int_{-1}^1 \dots \int_{-1}^1 \left| K(|u_{m-1} - u_m|) \right| \dots \left| K(|u - u_1|) \right| du_m \dots du_1 \right] \quad (22c)$$

Thus the current density is expressed as

$$J(u) = \lim_{n \rightarrow \infty} J_n(u) \quad (22d)$$

provided the series in equation (22c) converges as  $n \rightarrow \infty$ . The range of convergence for this series will be discussed later.

It is instructive to note that to zeroth order the current density  $J_0(u)$  is assumed to be uniform over the width of the film. The first-order correction to this assumption is included in  $J_1(u)$  and is computed by considering the sum of the interactions of all the source points in the films on a particular observation point. This sum

$$\lambda \int_{-1}^1 \left| K(|u - u_1|) \right| du_1 = \lambda \left| \kappa(u) \right| \quad (23)$$

where  $\kappa(u)$  will be referred to as the coupling factor. The second-order correction, contained within  $J_2(u)$ , is determined by considering the effect of all the source points on a particular source point before obtaining the coupling factor. The higher-order terms in  $\lambda$  are further expressions of the interactions of source points with source points.

It is noted that the terms in the kernel are of essentially two types:

$$\ln \left| a^2 \left( \frac{d}{w} \right)^2 + (u - u')^2 \right| \quad (24a)$$

and

$$\frac{u - u'}{d/w} \tan^{-1} \frac{a(d/w)}{u - u'} \quad (24b)$$

The first term (expression (24a)) is easily integrated with respect to  $u'$ . If

$$v = u - u'$$

then

$$\begin{aligned} \int_{-1}^1 \ln \left| a^2 \left( \frac{d}{w} \right)^2 + (u - u')^2 \right| du' &= \int_{u-1}^{u+1} \ln \left| a^2 \left( \frac{d}{w} \right)^2 + v^2 \right| dv = v \ln \left| a^2 \left( \frac{d}{w} \right)^2 + v^2 \right| \\ &\quad - 2v + 2a \left( \frac{d}{w} \right) \tan^{-1} \left[ \frac{v}{a(d/w)} \right] \Bigg|_{u-1}^{u+1} = \ln \frac{\left| a^2 (d/w)^2 + (u+1)^2 \right|^{u+1}}{\left| a^2 (d/w)^2 + (u-1)^2 \right|^{u-1}} \\ &\quad - 4 + 2a \left( \frac{d}{w} \right) \left\{ \tan^{-1} \left[ \frac{u+1}{a(d/w)} \right] - \tan^{-1} \left[ \frac{u-1}{a(d/w)} \right] \right\} = A_1 \end{aligned} \quad (24c)$$

When integrating expression (24b) it is important to remember that the inverse tangents are restricted to their principal values; therefore,

$$\begin{aligned} \int_{-1}^1 \frac{u - u'}{d/w} \tan^{-1} \frac{a(d/w)}{u - u'} du' &= \frac{w}{d} \left\{ \int_{-1}^u (u - u') \tan^{-1} \left[ \frac{a(d/w)}{u - u'} \right] du' \right. \\ &\quad \left. + \int_u^1 (u' - u) \tan^{-1} \left[ \frac{a(d/w)}{u' - u} \right] du' \right\} = \frac{w}{2} \left\{ \int_{-1}^u (u - u') \left[ \frac{\pi}{2} - \tan^{-1} \frac{u - u'}{a(d/w)} \right] du' \right. \\ &\quad \left. + \int_u^1 (u' - u) \left[ \frac{\pi}{2} - \tan^{-1} \frac{u' - u}{a(d/w)} \right] du' \right\} = \frac{w}{d} \left\{ \frac{\pi}{2} \left[ \int_{-1}^u (u - u') du' - \int_u^1 (u - u') du' \right] \right. \\ &\quad \left. - \int_{-1}^1 (u - u') \tan^{-1} \left[ \frac{u - u'}{a(d/w)} \right] du' \right\} = (1 + u^2) \frac{w}{d} \frac{\pi}{2} - a^2 \frac{d}{w} \left[ \frac{1}{2} \left( \left( 1 + \left[ \frac{1+u}{a(d/w)} \right]^2 \right) \right. \right. \\ &\quad \left. \left. \times \tan^{-1} \left[ \frac{1+u}{a(d/w)} \right] + \left( 1 + \left[ \frac{1-u}{a(d/w)} \right]^2 \right) \tan^{-1} \left[ \frac{1-u}{a(d/w)} \right] \right) - \frac{1}{a(d/w)} \right] = A_2 \end{aligned} \quad (24d)$$

Thus

$$\kappa(u) = A_1 \Big|_{a=1} + \left(k - \frac{1}{2}\right) A_1 \Big|_{a=2k-1} - \left(k + \frac{1}{2}\right) A_1 \Big|_{a=2k+1} + 2A_2 \Big|_{a=1} + A_2 \Big|_{a=2k-1} - A_2 \Big|_{a=2k+1} \quad (24e)$$

where  $k = \ell/d$ .

It is useful at this point to examine some of the properties of  $\kappa(u)$ . Figure 5 shows the absolute magnitude of the kernel plotted against  $u'$  for various values of  $u$ . The

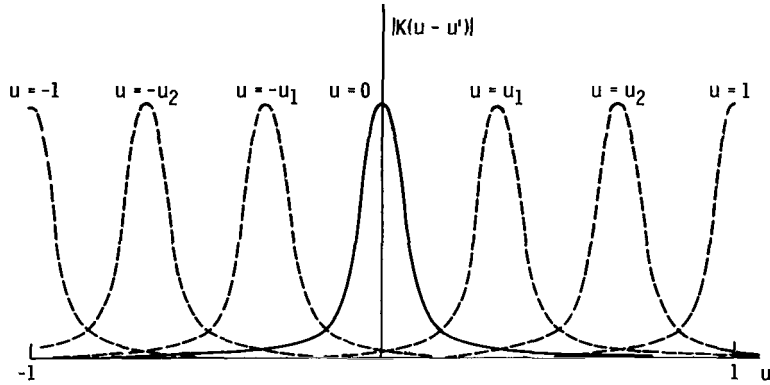


Figure 5. - Differential coupling factor (not to scale).

area under each curve is  $|\kappa(u)|$ . Since the kernel is negative definite,  $\kappa(u)$  is also negative definite. Due to the narrow effective width of the kernel (approximately  $10(\ell/w)$ ), it is seen that  $\kappa(u)$  is a weak function of  $u$  [ $\kappa(u) \approx \kappa(0)$ ] in the central region of the film. When  $u$  is within  $10(\ell/w)$  of the edge of the film,  $\kappa(u)$  is a strong function of  $u$ , and in fact it can be shown that at the edges

$$|\kappa(\pm 1)| = \frac{1}{2} |\kappa(0)| + \epsilon$$

where  $\epsilon$  is a small positive number. These observations are summarized in figure 6. Physically this implies that since an observation point is only affected by those source points within a range  $\approx 10(\ell/w)$ , the observation points which are not within  $10(\ell/w)$  of the edges are effectively in an infinitely wide film.

When a composite of figures 5 and 6 is considered, it is readily seen that

$$\int_{-1}^1 |\kappa(u_1)| |K(u - u_1)| du_1 \approx |\kappa(0)| |\kappa(u)| \quad (25a)$$

Thus, in general

$$\int_{-1}^1 \int_{-1}^1 \cdots \int_{-1}^1 \left| K(|u_{m-1} - u_m|) \right| \cdots \left| K(|u - u_1|) \right| du_m \cdots du_1 \approx \left| \kappa(0) \right|^{m-1} \left| \kappa(u) \right|$$

(25b)

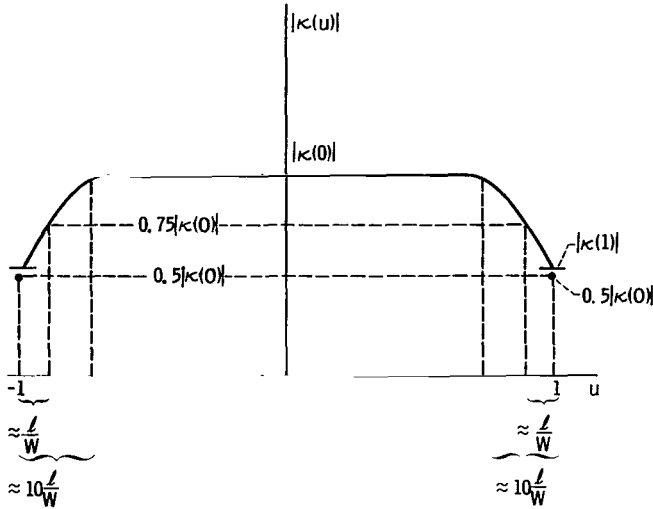


Figure 6. - Absolute value of coupling factor (not to scale).

Equations (25a) and (25b) are very nearly true in the central portion of the film. The error in these approximations, when  $u$  is within  $10(\ell/w)$  of the film edges, will be discussed in the next section. Combining equations (22) and (25) yields

$$J(u) = C \left( 1 - \lambda |\kappa(u)| \left\{ \sum_{n=0}^{\infty} (-1)^n [\lambda |\kappa(0)|]^n \right\} \right)$$

(26)

If  $\lambda |\kappa(0)| < 1$ , the series in equation (26) converges absolutely, and the current density distribution can be expressed in closed form as

$$J(u) = C \left[ 1 - \frac{\lambda |\kappa(u)|}{1 + \lambda |\kappa(0)|} \right]$$

(27)

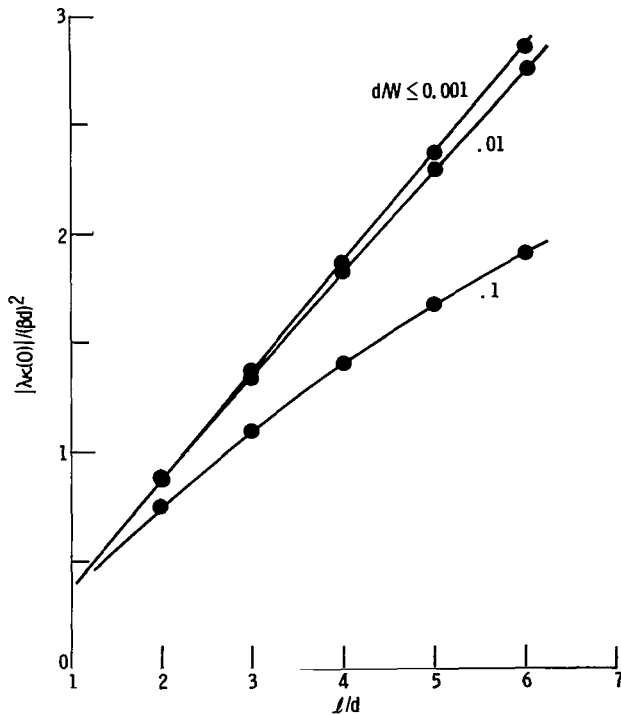


Figure 7. - Coupling factor magnitude.

Figure 7 indicates the range of values for the parameters  $d$ ,  $w$ , and  $\ell$  over which equation (26) converges. For example, once a film has been deposited  $\beta$ ,  $d$ , and  $w$  are fixed, and the range of convergence for equation (26) with  $\ell/d$  is to be determined. Clearly, the value of  $\ell/d$  cannot be less than or equal to 1, for this would

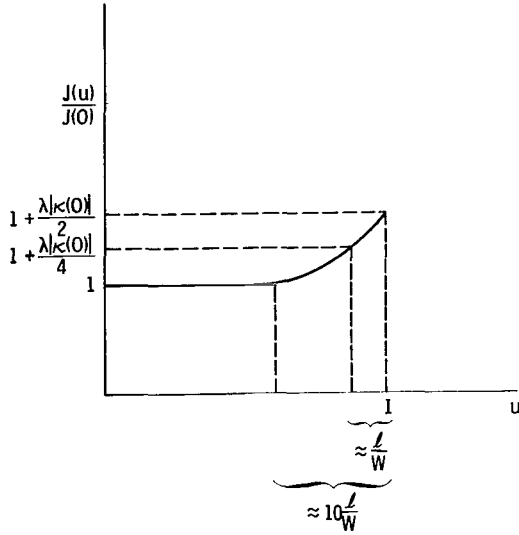


Figure 8. - Current distribution (not to scale).

imply that the two films touch or overlap. Since  $\lambda|\kappa(0)| < 1$ , the upper limit for  $\ell/d$  can be found by setting  $\lambda|\kappa(0)| = 1$ , dividing by  $(\beta d)^2$ , and finding that point on the appropriate  $d/w$  curve that has this value as its ordinate. The projection of this point on the  $\ell/d$  axis yields the upper critical value for  $\ell/d$ . Therefore  $1 < (\ell/d) < (\ell/d)_{cr}$ . Following somewhat similar lines, one can fix any two of  $d$ ,  $w$ , and  $\ell$  and determine the allowable values of the third parameter. If  $\lambda|\kappa(0)| \geq 1$ , the series does not converge and the Liouville-Neumann method is not applicable. With the help of figure 6 an approximate normalized sketch of  $J(u)$  against  $u$  can be drawn (fig. 8).

From equation (27) and the relation  $\vec{H} = \beta^{-2}(\nabla \times \vec{J})$ , the x-component of the magnetic field can be readily deduced:

$$H_x(u) = \frac{-1}{\beta^2} (\nabla \times \vec{J})_x = \frac{-1}{\beta^2} \frac{d}{dy} J(u) = \frac{-2}{\beta^2 w} \frac{d}{du} J(u) = \frac{2C\lambda}{\beta^2 w (1 + \lambda|\kappa(0)|)} \frac{d}{du} \left[ \int_{-1}^1 |K(|u - u'|)| du' \right] \quad (28)$$

Removing the absolute value signs from the kernel, applying Leibniz's rule, and remembering that

$$\frac{d}{du} f(u - u') = - \frac{d}{du'} f(u - u')$$

yield

$$H_x(u) = \frac{2C\lambda}{\beta^2 w (1 + \lambda|\kappa(0)|)} \int_{-1}^1 dK(|u - u'|) \quad (29)$$

$$H_x(u) = \left( \pm \frac{2C\lambda}{\beta^2 w} \right) \left[ \frac{K(|u - 1|) - K(|u + 1|)}{1 + \lambda|\kappa(0)|} \right] \quad (30)$$

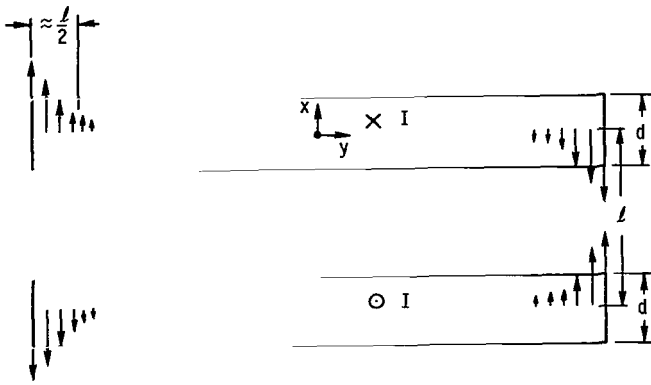


Figure 9. - Vertical component of magnetic field (not to scale).

where the plus and minus signs refer to the top and bottom films, respectively. An approximate sketch of equation (30) is given in figure 9.

In principle, Ampère's law can be used to evaluate  $H_y(x, u)$ ; however, for the purposes of the discussion in the next section, only the form of  $H_y$  is necessary. In the central portion of the films it can readily be seen that  $H_y$  is maximum at  $x = -(d/2)$ ,  $-[l - (d/2)]$  and approximately zero at  $x = (d/2)$ ,  $-[l + (d/2)]$ .

## ERROR ANALYSIS AND CONCLUSIONS

There are two sources of error in the analysis presented in the last section. The first error was introduced when it was assumed that the current density does not vary in the  $x$ -direction for the case  $(\beta d) \leq 1$  (one-dimensional approximation). The second error is associated with the approximations in equations (25a) and (25b) (the edge approximations).

### One-Dimensional Approximation

In order to evaluate this error it is convenient to use a self-consistency argument. In other words, the one-dimensional solution (eq. (27)) is resubstituted into the two-dimensional integral equation (eq. (17)) in order to find the  $x$ -direction variation of  $J$ . In practice, it is more convenient to use the differential counterpart of equation (17), namely  $\nabla^2 J = \beta^2 J$ . The  $x$ -direction variation is then used to find an improved  $y$ -direction variation. For the purposes of this report it is not important if  $J$  is not uniform in the  $x$ -direction, as long as the inclusion of this variation does not appreciably affect the  $y$ -direction variation. It is shown below that this is, in fact, the case.

From the behavior of the magnetic field in a superconducting film it can be argued that the largest  $x$ -direction variation of  $J$  occurs in the central portion of the film. This then is the worst region as far as an error in the one-dimensional approximation is concerned. Since both the current and the magnetic field satisfy linear differential equations of the same form, it follows that in the central portion of the films  $H_y(x)$  must be a solution of the equation

$$\frac{d^2 H_y(x)}{dx^2} = \beta^2 H_y(x) \quad (31a)$$

subject to the boundary conditions mentioned in the last section:

$$\left. \begin{aligned} H_y(x = +d/2) &\simeq 0 \\ H_y(x = -d/2) &\simeq J_w \end{aligned} \right\} \quad (31b)$$

It is easy then to show that in the central region of the film

$$H_y(x) = \frac{-J_w}{\sinh(\beta d)} \sinh \beta [x - (d/2)] \quad (31c)$$

Consequently,

$$J_z(x) = \frac{\partial H_y(x)}{\partial x} = J(0) \frac{\cosh \beta [x - (d/2)]}{\cosh \beta (d/2)} \quad (32)$$

It is seen that for  $(\beta d) = 1$ ,  $J\left(-\frac{d}{2}\right) \approx 1.5 J\left(\frac{d}{2}\right)$ . Thus there can be an appreciable x-direction variation.

Substituting equation (32) into equation (17) leads to an improved two-dimensional integral equation:

$$J(x, y) = C + \frac{\beta^2}{4\pi} \int_{-w/2}^{w/2} J(y') dy' \int_{-d/2}^{d/2} \frac{\cosh \beta [x' - (d/2)]}{\cosh(\beta d/2)} \ln \frac{|(x - x')^2 + (y - y')^2|}{|(x + x' + \ell)^2 + (y - y')^2|} dx' \quad (33)$$

To simplify comparison with the results obtained previously where  $J$  was assumed constant in the x-direction, it is advantageous to set  $x$  equal to zero in the integration over  $x'$ . Furthermore, it is clear that the largest contributions to the kernel come from source points closest to the field points. Thus in this "worst" region it is helpful to set  $y = y'$  in an attempt to establish the upper and lower bounds for

$$\int_{-d/2}^{d/2} \frac{\cosh \beta[x' - (d/2)]}{\cosh(\beta d/2)} \ln \frac{x'^2}{(\ell + x')^2} dx' \quad (34)$$

Since every function can be expressed as the sum of its even and odd parts, expression (34) can be rewritten as

$$\int_{-d/2}^{d/2} \cosh(\beta x') \ln \frac{x'^2}{\ell^2 - (x')^2} dx' + \int_{-d/2}^{d/2} (-1) \tanh\left(\frac{\beta d}{2}\right) \sinh(\beta x') \ln \left(\frac{\ell - x'}{\ell + x'}\right) dx' \quad (35)$$

Examination of the integrand indicates that the second integral in expression (35) is always positive. If

$$f(x') = \frac{\cosh \beta[x' - (d/2)]}{\cosh(\beta d/2)}$$

and

$$g(x') = \ln \frac{x'^2}{(\ell + x')^2}$$

then the first integral in expression (35) is just  $\int_{-d/2}^{d/2} f_E(x')g_E(x')dx'$ , where  $f_E(x')$  and  $g_E(x')$  are the even parts of  $f(x')$  and  $g(x')$ , respectively. Similarly,  $f_O(x')$  and  $g_O(x')$  are the odd parts of  $f(x')$  and  $g(x')$ . If  $\bar{f}_E$  is the average value of  $f_E(x')$  in the interval  $-\frac{d}{2} \leq x' \leq \frac{d}{2}$ , then

$$f_E(x') = \bar{f}_E + m_E(x')$$

Thus, expression (35) can be rewritten as

$$\int_{-d/2}^{d/2} f(x')g(x')dx' = \bar{f}_E \int_{-d/2}^{d/2} g_E(x')dx' + \int_{-d/2}^{d/2} m_E(x')g_E(x')dx' + \text{positive term} \quad (36)$$

Examining each of the integrands reveals that

$$\int_{-d/2}^{d/2} f(x')g(x')dx' < 0 \quad (37a)$$

$$\int_{-d/2}^{d/2} g_E(x')dx' < 0 \quad (37b)$$

$$\int_{-d/2}^{d/2} m_E(x')g_E(x')dx' > 0 \quad (37c)$$

Thus,

$$\int_{-d/2}^{d/2} f(x')g(x')dx' > \bar{f}_E \int_{-d/2}^{d/2} g_E(x')dx' \quad (38)$$

Since

$$\int_{-d/2}^{d/2} g_0(x')dx' = 0$$

and  $g(x')$  is always  $< 0$ , expression (38) yields

$$\int_{-d/2}^{d/2} f(x')|g(x')|dx' < \bar{f}_E \int_{-d/2}^{d/2} |g(x')|dx' = \frac{\sinh(\beta d/2)}{\beta d/2} \int_{-d/2}^{d/2} |g(x')|dx' \quad (39)$$

In a similar manner the lower bound can be found for

$$\int_{-d/2}^{d/2} f(x')|g(x')|dx'$$

The result is equal to expression (39) with  $[\sinh(\beta d/2)/(\beta d/2)]$  replaced by unity. Since  $\int_{-d/2}^{d/2} g(x/x', y/y')dx'$  can be identified with the kernel of the integral equation (eq.(19)), it follows that use of the self-consistency procedure yields an improved u-variation integral equation

$$J(u) = C - \alpha\lambda \int_{-1}^1 J(u') \left| K(|u - u'|) \right| du' \quad (40a)$$

where

$$1 < \alpha < \frac{\sinh \beta d/2}{\beta d/2} \quad (40b)$$

Thus, at worst,  $\alpha = 1.04$  (for the case  $\beta d = 1$ ) in the central region of the film. If  $\lambda$  is replaced by  $\alpha\lambda$  in the closed form solution, the magnitude of  $J(u)$  in the central region is less than 2 percent smaller than that predicted by equation (27). As was pointed out previously, this error is less near the film edges.

### Edge Approximation

It would appear from figure 6 that while the approximation  $\kappa(u) \approx \kappa(0)$  is a reasonable one to make in the central region of the film, its validity, as well as its usefulness at the edges, is questionable. Though the closed-form solution might therefore not be strictly true near  $u = \pm 1$ , equation (27) could be used as a reasonable trial function in an attempt to obtain a numerical solution for the one-dimensional integral equation.

Numerical solutions were obtained in this manner with the aid of an IBM 7094II computer. The results revealed that the greatest error in the closed form solution occurred for  $k \approx k_c$ , where  $J(\pm 1)$  was approximately 10 percent smaller than the value given by equation (27) for films with the same parameter values. It should be noted however that for cases where  $k \leq 0.65 k_c$ , this discrepancy is reduced to less than 5 percent.

If it is assumed that the superconducting films switch to the normally conducting state when  $J$  at any point in the films exceeds a critical value  $J_c$ , it is apparent that the switching is initiated at the film edges. From the error analysis it is clear that if the  $J(u)$  given in equation (27) is used to calculate a critical current  $I_c$  (in terms of  $J_c$ ), this value for the critical current will be smaller than the true critical current by less than 10 percent. It is noted that in calculating  $I_c$  the x-direction variation of  $J$  in the central portion of the film should be taken into account. This is easily done by combining equations (27) and (32) as is done in the sample critical current calculation shown in the appendix. The critical current density can be determined by making use of a microscopic theory (ref. 7) and/or by experimentally determining  $I_c$  for a particular choice of parameters which lie in the range treated in this report. Once  $J_c$  is known,  $I_c$  can be determined by using the above calculations for any other set of parameters which lie in the range under consideration in this report.

Lewis Research Center,  
National Aeronautics and Space Administration,  
Cleveland, Ohio, December 6, 1965.

## APPENDIX - SAMPLE CRITICAL CURRENT CALCULATION

The critical current  $I_c$  of a superconducting strip transmission line, for the case  $d/w \ll 1$ , can easily be calculated. For this case, the current is uniform over a very large percentage of the film width so that from equation (32) it can be shown that

$$I \approx J(0) w (\beta^{-1}) 2 \sinh(\beta d/2) \quad (A1)$$

The dimensionless variable  $u$  will not be used in this section. From equation (27), and making use of the fact that  $|\kappa(\pm w/2)| \approx \frac{1}{2} |\kappa(0)|$ , it can be seen that for  $\lambda |\kappa(0)| < 1$

$$\frac{J\left(y = \pm \frac{w}{2}\right)}{J(0)} \approx 1 + \frac{1}{2} \lambda |\kappa(0)| \quad (A2)$$

where the variation of  $J$  in the  $x$ -direction at the film edges has been neglected in line with the discussion in the last section. According to the critical current density hypothesis,  $I = I_c$  where  $J(\pm w/2) = J_c$ . Using this hypothesis and combining equations (A1) and (A2) yield

$$I_c = \frac{J_c w (\beta^{-1}) 2 \sinh(\beta d/2)}{1 + \frac{1}{2} \lambda |\kappa(0)|} \quad (A3)$$

The numerator of the right-hand side of equation (A3) is the critical current  $I_{cu}$  calculated on the assumption that the current density is uniform in the  $y$ -direction. It can be seen from equation (24) that

$$\left[ \lambda |\kappa(0)| \right]_{d/w \ll 1} \approx \frac{(\beta d)^2}{2} \left( \frac{\ell}{d} - \frac{1}{4} \right) \quad (A4)$$

From figure 8 it is evident that equation (A4) is satisfied for the case  $d/w \leq 0.001$ . It is interesting to note that in this range  $\lambda \kappa(0)$  is independent of  $(d/w)$ . Therefore,

$$\frac{I_c}{I_{cu}} \approx \left[ 1 + \frac{(\beta d)^2}{4} \left( \frac{\ell}{d} - \frac{1}{4} \right) \right]^{-1} \quad (A5)$$

For situations in which  $(d/w)$  is not much less than unity, equations (A1) and (A4) are not valid. In these cases the general expressions describing the variation of current density in the films can be used to calculate the critical current.

## REFERENCES

1. Swihart, James C. : Field Solution for a Thin-Film Superconducting Strip Transmission Line. *J. Appl. Phys.*, vol. 32, no. 3, Mar. 1961, pp. 461-469.
2. Meyers, Norman H. : Inductance in Thin-Film Superconducting Structures. *Proc. IRE*, vol. 49, no. 11, Nov. 1961, pp. 1640-1649.
3. Brennemann, A. E. : The In-Line Cryotron. *Proc. IEEE*, vol. 51, no. 3, Mar. 1963, pp. 442-451.
4. Brennemann, A. E. ; McNichol, J. J. ; and Seraphim, D. P. : Delay Times for Switching In-Line Cryotrons. *Proc. IEEE*, vol. 51, no. 7, July 1963, pp. 1009-1014.
5. Sass, A. R. : Image Properties of a Superconducting Ground Plane. *J. Appl. Phys.*, vol. 35, no. 3, pt. 1, Mar. 1964, pp. 516-521.
6. Sass, A. R. ; and Friedlaender, F. J. : Superconducting-to-Normally Conducting Transitions in Strip Transmission Line Structures. *J. Appl. Phys.*, vol. 35, no. 5, May 1964, pp. 1494-1500.
7. Bardeen, John: Critical Fields and Currents in Superconductors. *Rev. Mod. Phys.*, vol. 34, no. 4, Oct. 1962, pp. 667-681.
8. Cooper, Leon N. : Current Flow in Thin Superconducting Films. 7th International Conference on Low Temperature Physics, B. M. Graham and A. C. Hollis, eds., University of Toronto Press (Canada), 1961, pp. 416-418.
9. Marcus, Paul M. : Currents and Fields in a Superconducting Film Carrying a Steady Current. 7th International Conference on Low Temperature Physics, B. M. Graham and A. C. Hollis, eds., University of Toronto Press (Canada), 1961, pp. 418-421.
10. Anon. : Project Lightning. Final Report, Jan. 1959-May 1960, vol. 1, (ASTIA No. AD250676), International Business Machine Corp. May 31, 1960, pp. 9-13.

*"The aeronautical and space activities of the United States shall be conducted so as to contribute . . . to the expansion of human knowledge of phenomena in the atmosphere and space. The Administration shall provide for the widest practicable and appropriate dissemination of information concerning its activities and the results thereof."*

—NATIONAL AERONAUTICS AND SPACE ACT OF 1958

## NASA SCIENTIFIC AND TECHNICAL PUBLICATIONS

**TECHNICAL REPORTS:** Scientific and technical information considered important, complete, and a lasting contribution to existing knowledge.

**TECHNICAL NOTES:** Information less broad in scope but nevertheless of importance as a contribution to existing knowledge.

**TECHNICAL MEMORANDUMS:** Information receiving limited distribution because of preliminary data, security classification, or other reasons.

**CONTRACTOR REPORTS:** Technical information generated in connection with a NASA contract or grant and released under NASA auspices.

**TECHNICAL TRANSLATIONS:** Information published in a foreign language considered to merit NASA distribution in English.

**TECHNICAL REPRINTS:** Information derived from NASA activities and initially published in the form of journal articles.

**SPECIAL PUBLICATIONS:** Information derived from or of value to NASA activities but not necessarily reporting the results of individual NASA-programmed scientific efforts. Publications include conference proceedings, monographs, data compilations, handbooks, sourcebooks, and special bibliographies.

*Details on the availability of these publications may be obtained from:*

SCIENTIFIC AND TECHNICAL INFORMATION DIVISION  
NATIONAL AERONAUTICS AND SPACE ADMINISTRATION  
Washington, D.C. 20546